

MARS' OLDEST AND LARGEST CALDERA PITYUSA PATERA – UNIQUE DEPOSITS HINT AT MAGMA CHAMBER AT CRUST-MANTLE BOUNDARY

H. Bernhardt¹, D. A. Williams¹, C. Klimczak².
¹School of Earth and Space Exploration, Arizona State University, Tempe, USA (h.bernhardt@asu.edu); ²Structural Geology and Geomechanics Group, Department of Geology, University of Georgia, Athens, USA.

Introduction: Pityusa Patera (Fig. 1A) in the southern Malea Planum region (MPR) might be the largest ($\varnothing \sim 230$ km [1]) and oldest (+3.8 Ga [2,3]) caldera, i.e., volcanic collapse structure, on Mars. Here we present our preliminary findings on Pityusa Patera's geomorphology, possible structure, and the geologic implications as part of an ongoing, comprehensive investigation of the entire MPR [4].

Geomorphology: Pityusa Patera is the southernmost of four paterae in the MPR, the others being (south to north) Malea ($\sim 300 \times 195$ km), Amphitrites ($\varnothing \sim 150$ km), and Peneus ($\varnothing \sim 130$ km). Except for the very unusual Orcus and Phison Paterae, the MPR paterae are the widest on Mars. Pityusa Patera has no clearly defined rim, but forms a broad, oval-shaped, ~ 1.5 km deep depression with inner wall slopes around 3° .

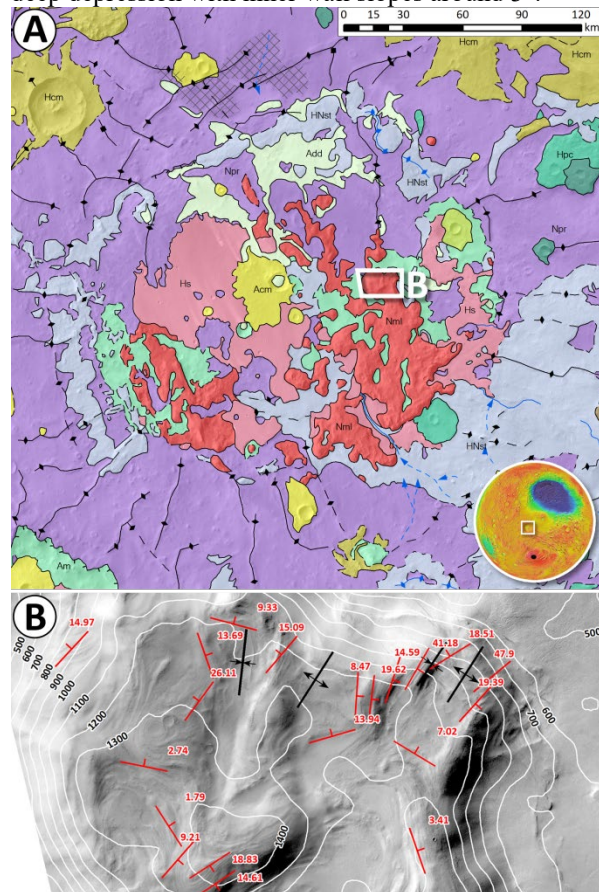


Figure 1: A) Excerpt of our photogeologic map of the MPR [4] showing Pityusa Patera. Unit *Nml* is red, unit *Npr* is purple. B) Cropped CTX image with 22 of the 57 bedding attitudes (red symbols) and 4 of 13 fold axes (black lines with converging/diverging arrows) that we obtained for unit *Nml*.

The patera is infilled by various materials (Fig. 1A) that include up to ~ 1.2 km high, rugged outcrops of

lobately lineated massifs (unit *Nml*) that do not occur in any other martian patera. The massifs of unit *Nml* cover $\sim 6,200$ km² and seem to be embayed by all adjacent units. Unit *Nml*'s lineations consist of up to few 10s of meters tall and wide ridges at an average spacing of ~ 150 m. The ridges form extensive, sub-parallel, lobate patterns including up to ~ 1.5 km wide circular and horseshoe-shaped arrangements. We interpret unit *Nml* as inselbergs, i.e., outcrops of material predating all surrounding materials, and its ridges to be the surface expressions of truncated, folded layers.

Tectonics: Using the *LayerTools* ArcMap add-in [5], we obtained 57 bedding attitudes (strikes & dips) of layers exposed within unit *Nml* via three-point measurements on HRSC topography and CTX image data (Fig. 1B). While dip angles of $>40^\circ$ occur, the median and average dips are $\sim 9^\circ$ and 12° , respectively; strikes show a weak trend towards NW-SE alignments. In two locations we were able to measure antithetic dips along fold trains, i.e., adjacent anti- and synforms (Fig. 1B). Assuming we were able to include the entire lengths of the folds, this enabled us to estimate the horizontal shortening strain $\epsilon_{(Nml)}$ to be ~ -1.2 to -2.2% .

As unit *Nml* exclusively occurs within Pityusa Patera and is embayed by, and thus predates, the surrounding wrinkle-ridged plains (unit *Npr*), we infer that the cause of the shortening that folded *Nml* was confined to the patera and unrelated to wrinkle ridge-formation. In accordance with previous findings [1-3], we interpret Pityusa Patera as a volcanic caldera formed by subsidence (via collapse of a magma chamber) and therefore usually bound by normal faults (which we propose are now covered by the wrinkle-ridged plains). Laboratory experiments, numeric models, as well as observations on Earth and Mars also indicate that interior caldera floors can remain intact and sag down as one lid or "plug" [e.g., 6-10]. For a "funnel-type" caldera that is bound by inward-dipping ring faults (Fig. 2), this plug is shortened according to the dip angle of the ring faults as it is sagging into a narrowing funnel during as well as after collapse (shallower dips will cause more shortening). In a simplified, axisymmetric case, this shortening can be expressed by $S = (2D)/(\tan \theta)$, where θ is the dip angle of the ring fault and D is the rim-to-floor depth of the caldera. Experiments and terrestrial observations have shown that θ for funnel-type calderas can be as shallow as $\sim 50^\circ$, although values $>60^\circ$ are more common [7,9-11]. The current depth of Pityusa Patera is ~ 1.5 km, although this is a minimum value due to

the substantial infill, including wrinkle-ridged plains material (unit *Npr*). In certain locations, unit *Npr* is indicated to be up to ~ 2.7 km thick by ghostcrater- and structural wrinkle ridge-analyses. For a range of $\theta = 50$ to 60° and $D = 1.5$ to 4.2 km, S would be ~ 0.9 to 7 km. Assuming the geographic extent of unit *Nml* across ~ 205 km to be the minimum diameter of the sagged plug, this results in a strain $\epsilon_{(plug)}$ of ~ -0.4 to -3.4% .

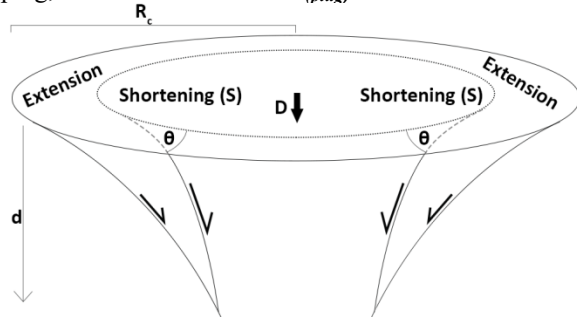


Figure 2: Schematic illustration of a funnel-type caldera structure including geometric parameters explained in the text.

Depth of the magma chamber: According to terrestrial observations [10,12,13], laboratory experiments [7,10], and numerical models [8,9,11], funnel-type calderas (Fig. 2) with inward-dipping ring faults tend to form above collapsing magma chambers whose roof depth d is larger than their radius. This geometry would create a radial compressive stress field in the interior plug of the caldera, which is in agreement with an earlier axisymmetric finite element model of the stress field in Zeus Patera, the oldest and largest of Olympus Mons' summit calderas [6]. Here, concentric ridges are found in the caldera center out to half its radius R_C , whereas the outer half hosts only concentric graben, thus indicating a transition from compressional to extensional stresses at $\sim 0.5 R_C$. The model showed that the surface stress is not strongly sensitive to the magma chamber's aspect ratio, internal pressure, or stiffness relative to its surroundings, but highly dependent on the radius and depth of the chamber. Therefore, this stress transition at a certain fraction of R_C can be used to estimate the depth d to the roof of the magma chamber (assuming its width to equal that of the caldera). For Pityusa Patera, the fraction of R_C at which surface stresses transition is not as straightforward to determine, but can be constrained by unit *Nml*, which our observations indicate to have undergone folding by a stress field that did not occur outside the caldera. Unit *Nml* extends up to ~ 100 km from the caldera center, for which we estimate a physiography-based best-fit radius R_C of ~ 115 km. This results in a radius fraction of ~ 0.86 , which, according to the model by [6], would correspond to a magma chamber depth d of $0.5 R_C = 57.5$ km. This should be regarded as a maximum estimate, as the magma chamber radius is assumed to equal that of the

caldera, but is likely smaller in a deep-seated funnel-type scenario [7,10,11].

Discussion & Conclusions: Pityusa Patera is unique not only because of its size and age, but also the exclusive occurrence of lobately lineated massifs (unit *Nml*). Interpreting these lineations to be surface expressions of folded layers, we estimated that *Nml* experienced a strain of $\epsilon_{(Nml)} \approx -1.2$ to -2.2% caused by a stress field that appears to have been confined to the patera. We suggest that this stress field was caused by the formation of the patera as a caldera, i.e., by subsidence initiated by the collapse of an underlying magma chamber. For a funnel-type setting (inward-dipping ring faults), we calculated that the plug at the center of the caldera floor would have experienced a strain of $\epsilon_{(plug)} \approx -0.4$ to -3.4% , thus being a viable scenario to explain unit *Nml* and $\epsilon_{(Nml)}$.

Using the axisymmetric finite element model by [6] and our mapping of unit *Nml*'s extent (as a proxy to ascertain the geographic extent of shortening within Pityusa Patera), we were also able to offer an maximum estimate of 57.5 km for the depth of the magma chamber whose collapse might have formed the patera. This depth would correspond to current crustal thickness models [14], which predict a moderate local thinning within Pityusa Patera to ~ 55 to 60 km. Although crustal thickness might have been different during patera formation at ≥ 3.8 Ga, models suggest it has not changed much within the last ~ 4 Ga [e.g., 15], therefore putting the Pityusa magma chamber at the crust-mantle boundary. This contrasts with Olympus Mons or comparable volcanoes on Earth such as Hawaii, whose magma chambers were estimated to be within the edifice, i.e., at depths of ≤ 16 km [e.g., 6]. Terrestrial crust-mantle-boundary magma chambers with attributed surface activity have been suggested for some volcanoes of the Cascades in northern California [16]. Here, olivine tholeiites are created at ~ 36 to 66 km depth, possibly a result of mantle flows being deflected by the underlying subducting slab of the Farallon plate. As for Pityusa Patera, an up to ~ 57.5 km deep magma chamber that is collapsing via depressurization (and thus likely feeding surface activity) would be in good agreement with predicted mantle-fed volcanism facilitated by deep ring fractures and mantle upwelling caused by the Hellas impact event [e.g., 3,17]. If unit *Nml* represents deposits (e.g., ignimbrites) derived from such a mantle source, good hyperspectral CRISM observations revealing corresponding signatures (e.g., high-Mg olivine) that are spatially associated with *Nml*'s layers could be vital to further this discussion.

References: [1] Head, J. W., & Pratt, S. (2001). LPSC#1627. [2] Bernhardt, H. et al. (2019). LPSC#1435; [3] Williams, D. A. et al. (2009). PSS, 57(8-9), 895-916. [4] Bernhardt, H., & Williams, D. A. (2019). Ann. M. of Plan. Geol. Mappers#7013. [5] Kneissl, T. et al. (2010). LPSC#1640 [6] Zuber, M. T., & Mouginis-Mark, P. J. (1992). JGR, 97(E11), 18295. [7] Roche, O. et al. (2000). JGR: Solid Earth, 105(B1), 395-416. [8] Kusumoto, S., & Takemura, K. (2003). GRLL, 30(24), 2-5. [9] Kusumoto, S., & Takemura, K. (2005). EPS, 57(11), e17-e20. [10] Howard, K. A. (2010). GSA Today, 20(10), 4-10. [11] Hardy, S. (2008). Geology, 36(12), 927. [12] Cole, J. et al. (2005). ESR, 69(1-2), 1-26. [13] Lipman, P. W. (1997). Bull. of Volcanology, 59(3), 198-218. [14] Parro, L. M. et al. (2017). Nature Scientific Reports, 7(1), 45629. [15] Breuer, D., & Spohn, T. (2003). JGR, 108(E7), 5072. [16] Elkins-Tanton, L. T. et al. (2001). Geology, 29(7), 631. [17] Peterson, J. E. (1978). LPSC, 3411-3432.